



Impaired adrenergic agonist-dependent beige adipocyte induction in obese mice

Woongchul SHIN¹⁾, Yuko OKAMATSU-OGURA^{1)*}, Shinya MATSUOKA¹⁾,
Ayumi TSUBOTA¹⁾ and Kazuhiro KIMURA¹⁾

¹⁾Laboratory of Biochemistry, Graduate School of Veterinary Medicine, Hokkaido University, Sapporo, Hokkaido 060-0818, Japan

ABSTRACT. Brown adipocytes, which exist in brown adipose tissue (BAT), are activated by adrenergic stimulation, depending on the activity of uncoupling protein 1 (UCP1). Beige adipocytes emerge from white adipose tissue (WAT) in response to chronic adrenergic stimulation. We investigated obesity-related changes in responses of both types of adipocytes to adrenergic stimulation in mice. Feeding of mice with high-fat diets (HFD: 45%-kcal fat) for 14 weeks resulted in significantly higher body and WAT weight compared to feeding with normal diets (ND: 10%-kcal fat). Injection with β 3-adrenergic receptor agonist CL316,243 (CL; 0.1 mg/kg, once a day) for one week elevated the mRNA and protein expression levels of UCP1 in BAT, irrespective of diet. In WAT, CL-induced UCP1 expression in ND mice; however, the responses to CL treatment were attenuated in HFD mice, indicating that CL-induced browning of WAT was impaired in obese mice. Flow cytometric analysis revealed a significant decrease in platelet-derived growth factor receptor (PDGFR) α -expressing beige adipocyte progenitors in WAT of HFD mice compared with those of ND mice. Expression of PDGF-B, a PDGFR α ligand, increased in WAT following CL-injection in ND mice, but not in HFD mice. Treatment of mice with a PDGFR inhibitor significantly decreased CL-dependent UCP1 protein induction in WAT. Our study demonstrates that β 3-adrenergic stimulation-dependent beige adipocyte induction in WAT is impaired by obesity in mice, potentially due to obesity-dependent reduction in the number of PDGFR α -expressing progenitors and decreased PDGF-B expression.

KEY WORDS: β 3-adrenergic receptor agonist, beige adipocytes, brown adipocytes, obesity, uncoupling protein 1

J. Vet. Med. Sci.

81(6): 799–807, 2019

doi: 10.1292/jvms.19-0070

Received: 1 February 2019

Accepted: 26 March 2019

Published online in J-STAGE:
8 April 2019

There are three types of adipocytes in mammals including brown, white, and beige adipocytes. White adipocytes store energy as triglyceride and release it in the form of fatty acids into circulation. In contrast, brown adipocytes utilize fatty acids as substrate for thermogenesis, which is mitochondrial uncoupling protein 1 (UCP1) dependent [4, 5, 12]. Beige adipocytes are inducible types of UCP1-expressing adipocytes that appear in white adipose tissue (WAT) under specific stimuli [9, 13, 30]. This change of the tissue is referred as “browning of WAT”, and adrenergic signaling pathway is recognized as a primary and dominant signal inducing browning [12].

Although beige adipocytes resemble brown adipocytes in terms of morphology and thermogenic function, they developmentally originate from a myogenic factor 5 (MYF5)-negative lineage, which also produces white adipocytes but not brown adipocytes [11]. In addition, beige adipocytes reportedly arise through the direct trans-differentiation of pre-existing white adipocytes in response to chronic cold exposure [2, 21]. In the absence of the stimulation, beige adipocytes are converted into unilocular white adipocytes accompanied by the degradation of mitochondria through mitophagy [1, 15]. In contrast, Wang *et al.* used AdiopoChaser mice to label mature adipocytes *in vivo*, and demonstrated that most beige adipocytes induced by cold exposure in subcutaneous WAT are derived from a progenitor population rather than from mature white adipocytes [33]. It has also been reported that stromal cells expressing platelet-derived growth factor receptor α (PDGFR α) can differentiate into both beige and white adipocytes in response to cold exposure and high-fat diet (HFD) feeding, respectively. Isolated PDGFR α -expressing cells were shown to differentiate into UCP1-expressing adipocyte by β 3-adrenergic stimulation *in vivo* [14]. Such results suggest that PDGFR α -positive cells in WAT are progenitors of beige adipocytes.

Interaction between platelet-derived growth factor (PDGF) dimer as a ligand and its receptor PDGFR regulates processes such as cell proliferation, cell migration, and cell differentiation in cells with a mesenchymal origin. Four different polypeptides are generated from four different genes (PDGF-A, PDGF-B, PDGF-C, and PDGF-D) [22], three homodimers (PDGF-AA, PDGF-BB,

*Correspondence to: Okamatsu-Ogura, Y.: y-okamatsu@vetmed.hokudai.ac.jp

©2019 The Japanese Society of Veterinary Science



This is an open-access article distributed under the terms of the Creative Commons Attribution Non-Commercial No Derivatives (by-nc-nd) License. (CC-BY-NC-ND 4.0: <https://creativecommons.org/licenses/by-nc-nd/4.0/>)

and PDGF-CC), and one heterodimer (PDGF-AB), which exclusively act through PDGFR α , while PDGF-DD activates PDGFR β [8, 22]. Binding of PDGF to the receptor induces the dimerization of the receptor, sequential activation of receptor tyrosine kinase, and autophosphorylation, which in turn activate downstream signal molecules such as phosphatidylinositol 3-kinase-protein kinase B/Akt (PI3K-Akt), Janus-activated kinase-Signal transducer-activated transcription (JAK-STAT), and phospholipase C [6, 8, 22]. It has recently been reported that PDGF-CC secreted from endothelial cells induce beige adipocytes in WAT, enhance whole body energy expenditure, and improve glucose tolerance in HFD-induced obese mice [27]. Therefore, the PDGF pathways could be involved in the browning of WAT through the regulation of PDGFR α -expressing progenitors in WAT. However, there is little information on the role of the PDGFs-PDGFR pathway in beige adipocyte induction.

The existence of functional BAT has been reported in adult humans [23], and the gene expression characteristics in human BAT more closely resemble those of murine beige adipocyte than brown adipocyte [28, 34]. The amount of human BAT is negatively correlated with adiposity and the amount declines with age [35]. We have previously reported that browning capacity in WAT declines with age, in addition to a reduction in the number of PDGFR α -positive cells [29]. Since aging is generally accompanied by the accumulation of WAT, we hypothesized that aging-dependent decreased browning capacity is attributed to obesity. In the present study, we investigated whether diet-induced obesity influences browning capacity and the number of PDGFR α -expressing progenitors in mice. In addition, to understand the mechanism of the regulation of the number of progenitors, the role of PDGF signaling was examined.

MATERIALS AND METHODS

Animals, treatment, and sampling

The experimental procedures and care of animals were approved by the Animal Care and Use Committee of Hokkaido University (Hokkaido, Japan). All experiments using mice were conducted in the animal facility approved by the Assessment and Accreditation of Laboratory Animal Care. Male C57BL/6J mice were housed in plastic cages in an air-conditioned room at 23°C with a 12:12 hr light:dark cycle. To examine the effect of obesity, 7-week-old mice were fed with high-fat diets (HFD; D12451, 45%-kcal fat, Research Diets, New Brunswick, NJ, U.S.A.) or a control diet (ND; D12450B, 10%-kcal fat, Research Diets) for 14 weeks. The mice were subcutaneously (SC) injected with β 3-adrenergic receptor agonist CL316,243 (CL; 0.1 mg/kg/day, once a day, American Cyanamid, Pearl River, NY, U.S.A.) for 1 week before sacrifice.

To examine the effect of the PDGFR inhibitor, mice were injected with imatinib mesylate (100 mg/kg/day, Fujifilm Wako Pure Chemical, Osaka, Japan) or saline for 10 days intraperitoneally (IP). From the fourth day of imatinib mesylate-injection, CL (0.1 mg/kg/day, SC) was simultaneously injected for 7 days.

After the treatments, mice were euthanized with carbon dioxide, and interscapular BAT and inguinal WAT quickly removed and transferred into liquid nitrogen for western blot analysis, RNAlater storage solution (Thermo Fisher Scientific, Waltham, MA, U.S.A.) for quantitative PCR analysis, 10% phosphate-buffered formalin for histological examination, and for stromal vascular (SV) fraction isolation and flow cytometry analysis.

Isolation of the SV fraction and flow cytometry analysis

Adipose tissue fragments were cut into small pieces and incubated in a Dulbecco's Modified Eagle Medium (DMEM) solution containing 2% fatty acid-free bovine serum albumin (Sigma-Aldrich Fine Chemical, St. Louis, MO, U.S.A.) and 2 mg/ml collagenase (Fujifilm Wako Pure Chemical) at 37°C for 2 hr with shaking at 100 cycles/min. The suspension was filtered through a 200- μ m nylon filter and centrifuged at $120 \times g$ for 5 min at room temperature. The pellets were suspended in ACK erythrocyte lysis buffer (150 μ M NH₄Cl, 10 mM KHCO₃, 1 mM EDTA-2Na). The sample was centrifuged at $120 \times g$ for 5 min at room temperature. The pellets were suspended in PBS containing 2% fetal calf serum. The number of SV cells were determined by counting the viable cells in a hemocytometer after staining cells with the Trypan blue dye.

Flow cytometry analysis

The SV fraction suspended in PBS containing 2% fetal calf serum was incubated with a mixture of antibodies containing either anti-CD31-PE-Cy (BioLegend, San Diego, CA, U.S.A.), anti-CD34-PE (BioLegend), anti-Sca1-PerCP/Cy5.5 (BioLegend), and anti-PDGFR α (CD140a)-APC (BioLegend) or containing anti-CD11c-FITC (BD Biosciences, San Jose, CA, U.S.A.), anti-CD206-PerCP/Cy5.5 (BioLegend), and anti-F4/80-APC (BioLegend) for 30 min on ice. After centrifuged at $1,000 \times g$ for 10 min at 4°C, the supernatant was discarded, and the pellet was suspended in PBS containing 2% FCS. The suspension was filtered through a 40 μ m nylon filter and analyzed on a flow cytometer (BD FACSVerser, BD Biosciences) with singlet discrimination to detect APC, PE-Cy, PE, and PerCP/Cy5.5 stained cells.

mRNA analysis

Total RNA was extracted using RNAiso reagent (Takara Bio, Shiga, Japan) according to the manufacturer's instructions. Total RNA (2 μ g) was reverse-transcribed using a 15-mer oligo (dT) adaptor primer and M-MLV reverse transcriptase (Promega, Madison, WI, U.S.A.). Real-time PCR was performed on a fluorescence thermal cycler (LightCycler system; Roche, Mannheim, Germany) using FastStart Essential DNA Green Master (Roche). Absolute expression levels were determined using a standard curve method with respective cDNA fragments as standards. The mRNA levels are expressed as relative values compared to β -actin mRNA levels. The primers used in the present study are listed in Table 1.

Table 1. Primer sequences for quantitative real-time PCR

Gene name (gene symbol): NCBI Reference Sequence number, Product size
Forward, and reverse primer sequence
Actb: NM_007393.5, 234 bp
5'-TCG TTA CCA CAG GCA TTG TGA T -3', 5'-TGC TCG AAG TCT AGA GCA AC -3'
<i>Ucp1</i> : NM_009463.3, 197 bp
5'-GTG AAG GTC AGA ATG CAA GC -3', 5'-AGG GCC CCC TTC ATG AGG TC -3'
<i>Cox4</i> : NM_009941.3, 252 bp
5'-TGA GCC TGA TTG GCA AGA GA -3', 5'-CGA AGC TCT CGT TAA ACT GG -3'
<i>Pgc1</i> : NM_008904.2, 214 bp
5'-GTG TGG AAC TCT CTG GAA CT -3', 5'-GCG TAC AAC TCA GAT TGC TC -3'
<i>Pdffa</i> : NM_008808.3, 386 bp
5'-GAG GGA TGG TAC TGA ATT TCG C -3', 5'-TGC AAA CTG CAG GAA TGG CT -3'
<i>Pdffb</i> : NM_011057.3, 94 bp
5'-ATG TGC CCT TCA GTC TGC TC -3', 5'-GAG ACA GGT CTC CTG CCC TA -3'
<i>Pdffc</i> : NM_019971.2, 178 bp
5'-GCC CGA AGT TTC CTC ATA CA -3', 5'-ACA CTT CCA TCA CTG GGC TC -3'
<i>Pdffd</i> : NM_027924.2, 167 bp
5'-CGA GGG ACT GTG CAG TAG AAA -3', 5'-TTG ATG GAT GCT CTC TGC GG -3'
<i>Adrb3</i> : NM_013462.3, 130 bp
5' -TTC CGT CGT CTT CTG TGT AG -3', 5'-GCG CAC CTT CAT AGC CAT CA -3'

Protein analysis

Tissue specimens were homogenized in Tris-EDTA buffer (10 mM Tris and 1 mM EDTA, pH 7.4). The samples were centrifuged at $800 \times g$ for 10 min at 4°C, and the fat-free supernatants were collected and used for protein concentration measurements and western blot analysis. For the western blot analysis, proteins were separated by SDS-PAGE and transferred to a polyvinylidene fluoride membrane (Immobilon; Millipore, Tokyo, Japan). After blocking the membrane with 5% skim milk (Morinaga Milk Industry Co., Tokyo, Japan), it was incubated with a primary anti-rat UCP1 antibody, a kind gift from Prof. Teruo Kawada (Kyoto University), an anti-bovine cytochrome oxidase complex 4 antibody (COX4; Molecular Probes, Eugene, OR, U.S.A.), or an anti- β -actin antibody (Sigma-Aldrich Fine Chemical) for 1 hr. The bound antibody was visualized using horseradish peroxidase-linked goat anti-rabbit immunoglobulin (Cell Signaling Technology, Danvers, MA, U.S.A.) for the detection of UCP1 and β -actin or horseradish peroxidase-linked goat anti-mouse immunoglobulin (Cell Signaling Technology) for the detection of COX4, and an enhanced chemiluminescence system (Millipore). Total UCP1 or COX4 contents (arbitrary unit per depot) were calculated by multiplying the protein amount detected by western blot (arbitrary unit per μg protein) by the total protein amount extracted from the whole depot (μg per depot).

Histology

Tissue specimens fixed in 10% formalin were embedded in paraffin, cut into 4- μm -thick sections, and the sections stained with hematoxylin and eosin. The stained samples were examined under a light microscope.

Data analysis

Values are expressed as means \pm SE. Statistical analyses were performed using Student's *t*-test or ANOVA followed by Tukey's *post-hoc* tests. All the statistical analyses were performed in IBM SPSS.

RESULTS

To examine the effect of HFD-induced obesity on beige adipocyte induction, mice were fed with normal diet (ND: 10%-kcal fat) or HFD (45%-kcal fat) for 14 weeks. HFD feeding led to higher body weight (36% higher than ND mice), and increased BAT and WAT weight (Fig. 1). The brown adipocytes in HFD mice had larger lipid droplets in the cytoplasm and the sizes of white adipocytes were also larger than those in ND mice (Fig. 2), suggesting diet-induced obesity. ND mice that received β 3-AR agonist, CL316,243 (CL)-injection for 1 week exhibited multilocular adipocytes in inguinal WAT (iWAT), suggesting the induction of beige adipocytes upon β 3-adrenergic stimulation (Fig. 2). However, the emergence of multilocular adipocytes in iWAT was significantly lower in HFD mice than in ND mice (Fig. 2).

To assess the degree of beige adipocyte induction in iWAT, the expression levels of *Ucp1* mRNA were investigated. Basal *Ucp1* mRNA expression levels in BAT in HFD mice were comparable with those in ND mice, and the levels increased approximately two-fold following CL-injection in both ND and HFD mice (Fig. 3A). Similar changes in the mRNA expression levels of cytochrome c oxidase 4 (COX4), a mitochondrial marker, were observed in BAT in both ND and HFD mice, while there were no alterations in the mRNA expression levels of peroxisome proliferator-activated receptor gamma coactivator 1-alpha (PGC1 α),

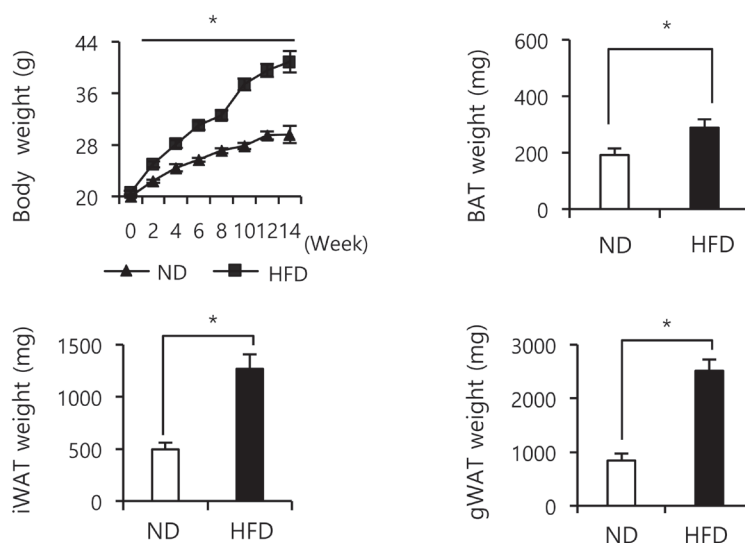


Fig. 1. Effects of normal or high-fat diet feeding on body weights and adipose tissue weight in mice. Seven week-old male C57BL/6J mice were fed on normal diets (ND: 10%-kcal fat) or high-fat diets (HFD: 45%-kcal fat). Body weights were measured every three weeks. After 14 weeks of feeding, interscapular brown adipose tissue (BAT), inguinal white adipose tissue (iWAT), and perigonadal white adipose tissue (gWAT) were excised and their weights were measured. Values are expressed as means \pm SE for 6 mice. * P <0.05 by Student's t -test.

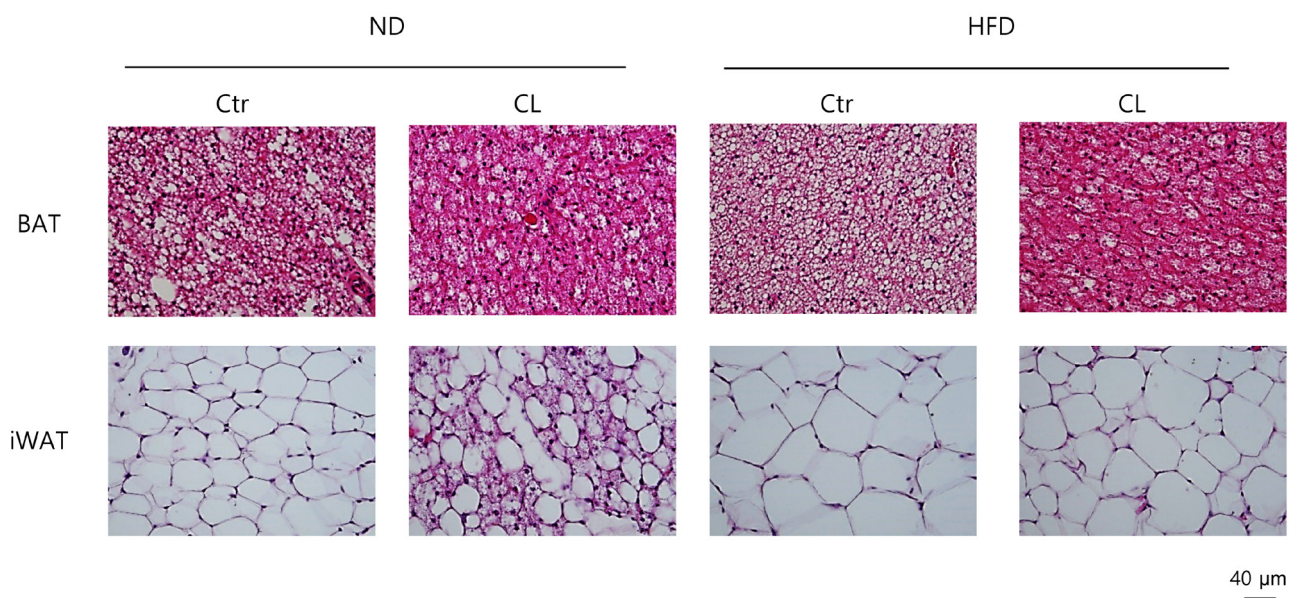


Fig. 2. Effect of β_3 -adrenergic agonist on adipose tissue morphological features in mice fed with normal or high-fat diets. The mice fed with normal diets (ND) or high-fat diets (HFD) were subcutaneously injected with β_3 -adrenergic receptor agonist CL316,243 (CL; 0.1 mg/kg/day, once a day) for 1 week. Illustrative images of the brown adipose tissue (BAT) and inguinal white adipose tissue (iWAT) sections of the control or CL-injected ND and HFD mice stained with hematoxylin and eosin are shown.

a transcriptional coactivator that regulates the expression of *Ucp1*, *Cox4*, and other mitochondria-related genes. In iWAT of ND mice, *Ucp1* mRNA expression was low at basal, but increased more than 8-fold following CL-injection, accompanied by increased expression of *Cox4* and *Pgc1a* (Fig. 3B). Nevertheless, the responses of the genes to CL-injection were markedly attenuated in HFD mice. Consistent with the mRNA expression levels, in BAT, CL-injection increased UCP1 and COX4 protein levels in ND and HFD mice similarly (Fig. 4A). In iWAT, CL-injection increased protein levels of UCP1 and COX4 in ND mice but did not influence the expression levels of the proteins in HFD mice. The results indicate that CL-dependent browning of iWAT was impaired in high-fat diet-induced obese mice.

To examine the underlying mechanism of the impairment of CL-dependent browning of iWAT in HFD mice, first we analyzed

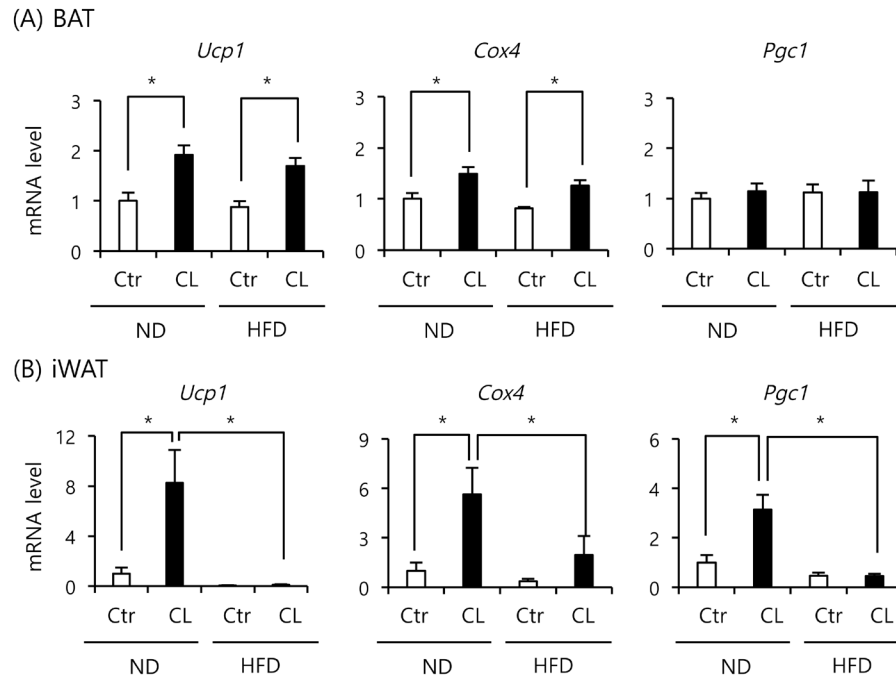


Fig. 3. Effect of β 3-adrenergic agonist on mRNA expression levels of *Ucp1*, *Cox4*, and *Pgc1* in the adipose tissues in mice fed with normal or high-fat diets. Expression levels of the genes in brown adipose tissue (A) and inguinal white adipose tissue (iWAT) (B) of the no-treatment control or the CL-injected normal diet (ND) and high-fat diet (HFD) mice were analyzed using quantitative real-time PCR. Data normalized to *Actb* expression are expressed as values relative to control ND mice. Values are expressed as means \pm SE for 4 mice. * $P < 0.05$ by ANOVA followed by Tukey's *post-hoc* tests.

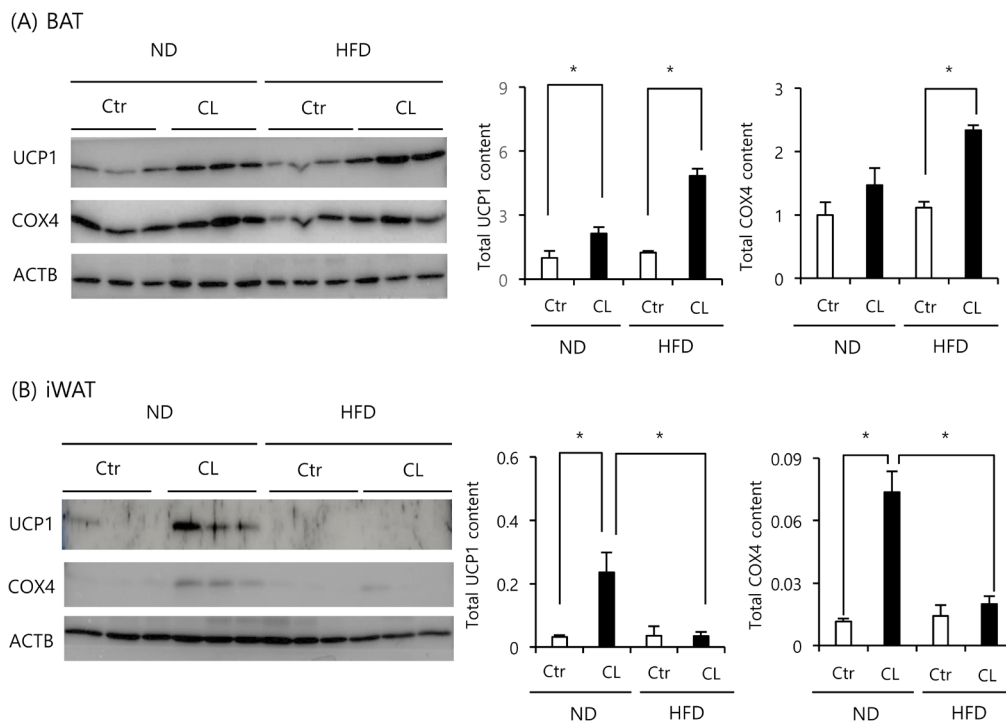


Fig. 4. Effect of β 3-adrenergic agonist on protein expression in the adipose tissues in mice fed with normal or high-fat diet. UCP1 and COX4 protein levels in brown adipose tissue (BAT) (A) and inguinal white adipose tissue (iWAT) (B) of no-treatment control or CL-injected normal diet (ND) and high-fat diet (HFD) mice were analyzed by western blotting using 5 μ g and 30 μ g of total protein extracted from BAT and iWAT, respectively. ACTB is shown as a loading control. Total contents of UCP1 and COX4 per depot were estimated by multiplying the protein amount detected by western blotting (arbitrary unit per μ g protein) by the total protein extracted from whole depot (μ g per depot), and expressed as values relative to the respective amounts in BAT of control ND mice. Values are expressed as means \pm SE for 5 mice. * $P < 0.05$ by ANOVA followed by Tukey's *post-hoc* tests.

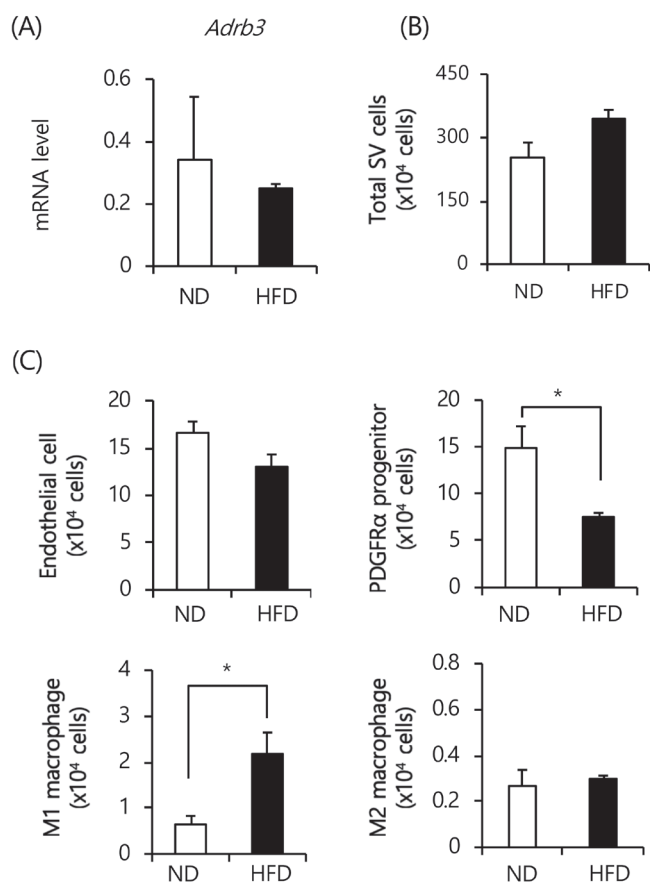


Fig. 5. Expression of *Adrb3* and the number of PDGFR α -expressing progenitors in the stromal-vascular fraction of inguinal white adipose tissue in mice fed with normal or high-fat diets. (A) Expression of *Adrb3* gene in inguinal white adipose tissue (iWAT) of the normal diet (ND) and high-fat diet (HFD) mice was analyzed using quantitative real-time PCR. Data are normalized to Actb expression. Total number (B) and composition (C) of cells in stromal-vascular (SV) fraction of iWAT was analyzed by flow cytometry. Comparison of endothelial cells (CD31+), PDGFR α -expressing progenitors (CD31-, CD34+, Sca1+, PDGFR α +), M1 macrophages (F4/80+, CD11c+, CD206-), and M2 macrophages (F4/80+, CD11c-, CD206+) between ND and HFD mice is shown. Values are expressed as means \pm SE for 4 mice. * P <0.05 by Student's *t*-test.

gene expression of β 3-adrenergic receptor, however, there was no significant difference between ND and HFD groups (Fig. 5A). Next, the amounts of PDGFR α -expressing progenitors in iWAT were analyzed. Although there was no significant difference in the number of SV cells in iWAT (Fig. 5B), flow cytometry analysis revealed that the number of PDGFR α -expressing progenitors in iWAT of HFD mice ($7.55 \pm 0.42 \times 10^4$ cells/depot) was significantly lower than that of ND mice ($1.49 \pm 0.12 \times 10^5$ cells/depot), while there was no significant difference in the number of endothelial cells between ND and HFD mice (Fig. 5C). As previously reported [24], M1 macrophages, but not M2 macrophages, were significantly higher in HFD mice ($2.20 \pm 0.50 \times 10^4$ cells/depot) than in ND mice ($0.60 \pm 0.10 \times 10^4$ cells/depot). The results suggest that browning capacity of WAT decreased in obese mice potentially due to the lower numbers of progenitors.

To evaluate the regulatory mechanism associated with the number of PDGFR α -expressing progenitors, the mRNA expression levels of *Pdgf* as ligands for PDGFR were determined. Among the *Pdgf* isoforms, *Pdgfb* and *Pdgfd* exhibited higher copy numbers of transcripts relative to *Pdgfa* and *Pdgfc*, and all the isoforms were not influenced by HFD feeding in iWAT (Fig. 6). In iWAT, mRNA expression of *Pdgfb* was significantly enhanced by CL-injection in ND mice, but there was no apparent change in mRNA expression in HFD mice. Therefore, it is plausible the CL-induced PDGF-B regulates the proliferation or the differentiation of PDGFR α -expressing progenitors, leading to the induction of beige adipocytes. To examine this possibility, mice were treated with a PDGFR inhibitor, imatinib mesylate [18, 19], together with CL. Although treatment with imatinib mesylate did not influence the number of PDGFR α -expressing progenitors in iWAT (Fig. 7A), it significantly suppressed CL-induced UCP1 expression but not COX4 expression (Fig. 7B).

DISCUSSION

In the present study, the effect of diet-induced obesity on β 3-adrenergic agonist-mediated browning of WAT was investigated in mice. HFD feeding resulted in obesity with increased fat accumulation, and almost completely abrogated CL-induced mRNA and protein expression of UCP1 and the emergence of multilocular adipocytes in iWAT. The results indicate that CL-dependent browning of WAT was impaired in diet-induced obese mice. Since it has also been reported that stromal cell expressing platelet-derived growth factor receptor α (PDGFR α) can differentiate into beige adipocytes [14], we examined the number of PDGFR α progenitors in iWAT of ND and HFD mice. The numbers of PDGFR α -expressing progenitors were reduced following HFD feeding. Therefore, it is likely that the reduction in the numbers of PDGFR α -expressing progenitors is an underlying mechanism for the attenuation of beige adipocyte development in obese mice. The mechanism for underlying the reduction in the numbers

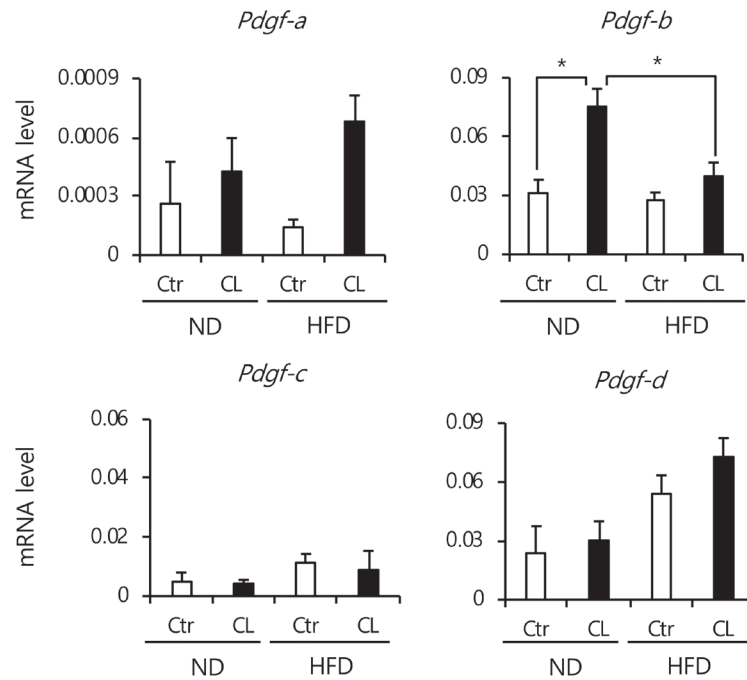


Fig. 6. Effect of β 3-adrenergic agonist on mRNA expression of Pdgf isoforms in the inguinal white adipose tissue in mice fed with normal or high-fat diet. Expression of *Pdgf* genes in inguinal white adipose tissue (iWAT) in the no-treatment control or CL-injected normal diet (ND) and high-fat diet (HFD) mice was analyzed using quantitative real-time PCR. Data normalized to *Actb* expression are expressed as means \pm SE for 4 mice. * P <0.05 by ANOVA followed by Tukey's *post-hoc* tests.

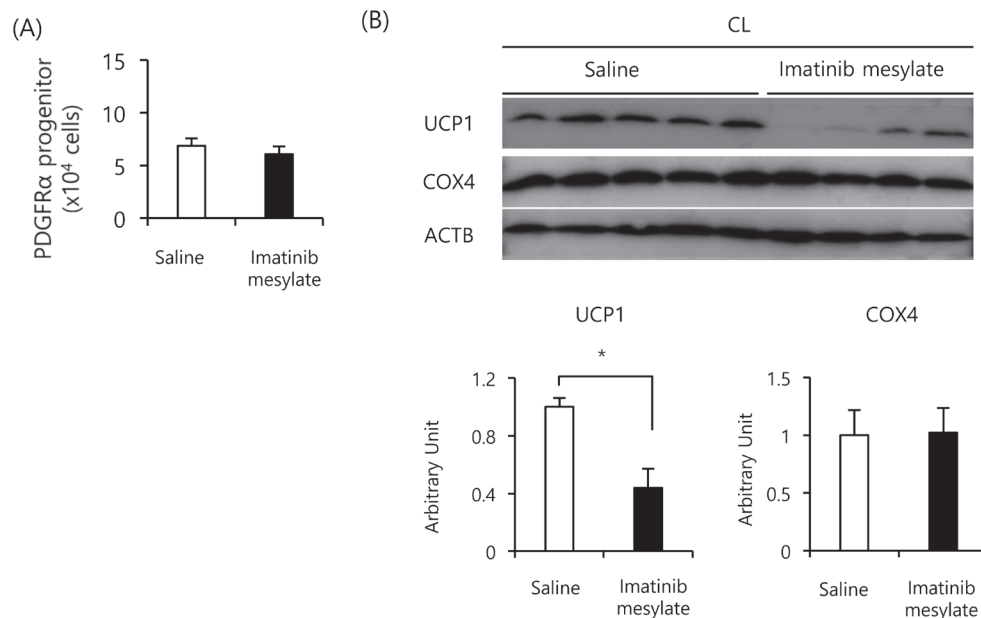


Fig. 7. Effect of PDGFR inhibitor on the number of PDGFR α -expressing progenitors and β 3-adrenergic agonist-dependent UCP1 expression in the inguinal white adipose tissue. Seven-week-old male C57BL/6J mice were intraperitoneally injected with saline or imatinib mesylate (100 mg/kg, once a day) for 10 days. From the fourth day of PDGFR inhibitor injection, CL (0.1 mg/kg, once a day) was also intraperitoneally injected for 6 days. (A) Cellular composition of the stromal-vascular (SV) fraction isolated from inguinal white adipose tissue (iWAT) was analyzed by flow cytometry as described in the legend of Fig. 5. (B) UCP1 and COX4 protein levels in iWAT of saline- or imatinib mesylate-injected mice were analyzed by western blotting using 30 μ g of total protein extracted from iWAT. ACTB is shown as a loading control. UCP1 and COX4 protein expression levels are expressed as values relative to those of the saline-injected mice. Values are expressed as means \pm SE for 5–6 mice. * P <0.05 by Student's *t*-test.

of progenitors in obese mice was unknown. However, since it has been reported that PDGFR α progenitors have the capacity to differentiate into both beige and white adipocytes in response to cold exposure and HFD feeding, respectively [14], it is plausible that more PDGFR α progenitors differentiated into white adipocytes than beige adipocytes following HFD feeding in the present study. Further studies would be required to determine the precise mechanism underlying the reduction in the numbers of PDGFR α progenitors.

In contrast to WAT, the response of BAT to CL injection was not altered in HFD mice. The reason for this difference between WAT and BAT is not clear, however, beige adipocytes are distinct from brown adipocytes in developmental origin and gene expression pattern [11]. Also, it was reported that beige adipocytes have a significant impact on whole body glucose [7] and lipid [3] homeostasis. Thus, it is likely that distinctive role of brown and beige adipocytes in metabolism might be associated with the difference in their responses to CL injection in diet-induced obese mice.

Pdgfb mRNA expression in iWAT of mice fed with ND increased in response to CL-injection, and the expression levels were significantly lower in obese mice, while mRNA expression levels in the other three *Pdgf* isoforms were unaffected by the differences in diets and in CL or saline-injection in iWAT. In addition, *Pdgfb* mRNA expressed higher copy numbers of transcripts than *Pdgfa* and *Pdgfc* in iWAT, while *Pdgfd* mRNA expressed comparable copy numbers with *Pdgfb*. It should be noted that three homodimers, PDGF-AA, PDGF-BB, and PDGF-CC, and one heterodimer, PDGF-AB, constitute the ligands for PDGFR α , while PDGF-DD is the ligand for PDGFR β [6, 22]. In addition, injection of PDGFR inhibitor considerably suppressed CL-induced UCP1 protein expression in iWAT without influencing the number of PDGFR α progenitors. Consistent with the above results, PDGF-BB enhances adipogenesis of orbital fibroblasts by enhancing the mRNA expression of peroxisome proliferator-activated receptor γ (PPAR γ), a master regulator of adipogenesis [32] and a potent inducer of beige adipocytes through the stabilization of PRD1-BF-1-RIZ1 homologous-domain-containing protein-16 (PRDM16) [21]. Therefore, although it has recently been reported that PDGF-CC secreted from endothelial cell induces beige adipocytes in WAT [27], the results of the present study highly suggest that PDGF-B is the β -adrenergic agonist-regulated dominant effector ligand for PDGFR α among the PDGF isoforms in iWAT for the induction of beige adipocyte differentiation, without influencing the progenitor recruitment, and that attenuated responses of *Pdgfb* mRNA expression levels to adrenergic stimulation in obese state is one of the potential causes of the decreased beige adipocyte development.

It was observed that the number of M1 but not M2 macrophages increased in iWAT following HFD feeding. Macrophages have a critical and opposite role in the induction of beige adipocytes. Anti-inflammatory resident M2 macrophages are reportedly induce beige adipocytes by synthesizing norepinephrine (NE) in response to cold stimulation [10, 20]. Conversely, pro-inflammatory M1 macrophages migrated into obese WAT suppress beige adipocyte induction in response to cold stimulation [16, 25]. In addition, accumulated fat is associated with abnormal expression of adipokines and chronic low-grade inflammation due to the macrophage infiltration [26], which may contribute to the attenuation of beige adipocyte induction. In fact, cold-induced *Ucp1* mRNA expression is downregulated in WAT, accompanied by an increase in the expression levels of TNF α , MCP-1, and other inflammation markers in obese mice [17]. In addition, UCP1 expression induced by adrenergic receptor agonist, isoproterenol, in C3H10T1/2 adipocytes, is suppressed under co-culture with RAW264.7 macrophages [24]. Therefore, increased infiltration of M1 macrophage in iWAT may also facilitate the attenuated browning of WAT in obese mice.

In summary, our study demonstrates that β 3-adrenergic stimulation-dependent beige adipocyte development in WAT is impaired by obesity in mice, while brown adipocyte development through β 3-adrenergic receptor is unaltered. The impairment is most likely due to obesity-dependent reduction in the number of PDGFR α -expressing progenitors and decreased PDGF-B expression. Our study could have implications for the obesity-dependent decline in human brown fat [31, 35] and the development of therapeutic strategies for the management of obesity.

ACKNOWLEDGMENTS. We thank Dr. Teruo Kawada (Kyoto University) for the kind gift of the anti-UCP1 antibody. This study was supported by JSPS KAKENHI Grant Numbers 17K08118 and 18H02274, and Grants-in-Aid for the Naito Foundation.

REFERENCES

1. Altshuler-Keylin, S., Shinoda, K., Hasegawa, Y., Ikeda, K., Hong, H., Kang, Q., Yang, Y., Perera, R. M., Debnath, J. and Kajimura, S. 2016. Beige adipocyte maintenance is regulated by autophagy-induced mitochondrial clearance. *Cell Metab.* **24**: 402–419. [Medline] [CrossRef]
2. Barbatelli, G., Murano, I., Madsen, L., Hao, Q., Jimenez, M., Kristiansen, K., Giacobino, J. P., De Matteis, R. and Cinti, S. 2010. The emergence of cold-induced brown adipocytes in mouse white fat depots is determined predominantly by white to brown adipocyte transdifferentiation. *Am. J. Physiol. Endocrinol. Metab.* **298**: E1244–E1253. [Medline] [CrossRef]
3. Bartelt, A., Bruns, O. T., Reimer, R., Hohenberg, H., Ittrich, H., Peldschus, K., Kaul, M. G., Tromsdorf, U. I., Weller, H., Waurisch, C., Eychmüller, A., Gordts, P. L., Rinninger, F., Bruegelmann, K., Freund, B., Nielsen, P., Merkel, M. and Heeren, J. 2011. Brown adipose tissue activity controls triglyceride clearance. *Nat. Med.* **17**: 200–205. [Medline] [CrossRef]
4. Calderon-Dominguez, M., Mir, J. F., Fucho, R., Weber, M., Serra, D. and Herrero, L. 2015. Fatty acid metabolism and the basis of brown adipose tissue function. *Adipocyte* **5**: 98–118. [Medline] [CrossRef]
5. Cannon, B. and Nedergaard, J. 2004. Brown adipose tissue: function and physiological significance. *Physiol. Rev.* **84**: 277–359. [Medline] [CrossRef]
6. Chen, P. H., Chen, X. and He, X. 2013. Platelet-derived growth factors and their receptors: structural and functional perspectives. *Biochim. Biophys. Acta* **1834**: 2176–2186. [Medline] [CrossRef]
7. Chen, Y., Ikeda, K., Yoneshiro, T., Scaramozza, A., Tajima, K., Wang, Q., Kim, K., Shinoda, K., Sponton, C. H., Brown, Z., Brack, A. and Kajimura, S. 2019. Thermal stress induces glycolytic beige fat formation via a myogenic state. *Nature* **565**: 180–185. [Medline] [CrossRef]

8. Choudhury, G. G., Marra, F., Kiyomoto, H. and Abboud, H. E. 1996. PDGF stimulates tyrosine phosphorylation of JAK 1 protein tyrosine kinase in human mesangial cells. *Kidney Int.* **49**: 19–25. [[Medline](#)] [[CrossRef](#)]
9. Harms, M. and Seale, P. 2013. Brown and beige fat: development, function and therapeutic potential. *Nat. Med.* **19**: 1252–1263. [[Medline](#)] [[CrossRef](#)]
10. Hui, X., Gu, P., Zhang, J., Nie, T., Pan, Y., Wu, D., Feng, T., Zhong, C., Wang, Y., Lam, K. S. and Xu, A. 2015. Adiponectin enhanced cold-induced browning of subcutaneous adipose tissue via promoting M2 macrophage proliferation. *Cell Metab.* **22**: 279–290. [[Medline](#)] [[CrossRef](#)]
11. Ikeda, K., Maretich, P. and Kajimura, S. 2018. The common and distinct features of brown and beige adipocytes. *Trends Endocrinol. Metab.* **29**: 191–200. [[Medline](#)] [[CrossRef](#)]
12. Kajimura, S. and Saito, M. 2014. A new era in brown adipose tissue biology: molecular control of brown fat development and energy homeostasis. *Annu. Rev. Physiol.* **76**: 225–249. [[Medline](#)] [[CrossRef](#)]
13. Kajimura, S., Spiegelman, B. M. and Seale, P. 2015. Brown and beige fat: physiological roles beyond heat generation. *Cell Metab.* **22**: 546–559. [[Medline](#)] [[CrossRef](#)]
14. Lee, Y. H., Petkova, A. P., Mottillo, E. P. and Granneman, J. G. 2012. In vivo identification of bipotential adipocyte progenitors recruited by β 3-adrenoceptor activation and high-fat feeding. *Cell Metab.* **15**: 480–491. [[Medline](#)] [[CrossRef](#)]
15. Lu, X., Altshuler-Keylin, S., Wang, Q., Chen, Y., Henrique Sponton, C., Ikeda, K., Maretich, P., Yoneshiro, T. and Kajimura, S. 2018. Mitophagy controls beige adipocyte maintenance through a Parkin-dependent and UCP1-independent mechanism. *Sci. Signal.* **11**: eaap8526. [[Medline](#)]
16. Machida, K., Okamatsu-Ogura, Y., Shin, W., Matsuoka, S., Tsubota, A. and Kimura, K. 2018. Role of macrophages in depot-dependent browning of white adipose tissue. *J. Physiol. Sci.* **68**: 601–608. [[Medline](#)] [[CrossRef](#)]
17. Martins, F. F., Bargut, T. C. L., Aguila, M. B. and Mandarim-de-Lacerda, C. A. 2017. Thermogenesis, fatty acid synthesis with oxidation, and inflammation in the brown adipose tissue of ob/ob (-/-) mice. *Ann. Anat.* **210**: 44–51. [[Medline](#)] [[CrossRef](#)]
18. Matei, D., Chang, D. D. and Jeng, M. H. 2004. Imatinib mesylate (Gleevec) inhibits ovarian cancer cell growth through a mechanism dependent on platelet-derived growth factor receptor alpha and Akt inactivation. *Clin. Cancer Res.* **10**: 681–690. [[Medline](#)] [[CrossRef](#)]
19. McGary, E. C., Onn, A., Mills, L., Heimberger, A., Eton, O., Thomas, G. W., Shtivelband, M. and Bar-Eli, M. 2004. Imatinib mesylate inhibits platelet-derived growth factor receptor phosphorylation of melanoma cells but does not affect tumorigenicity in vivo. *J. Invest. Dermatol.* **122**: 400–405. [[Medline](#)] [[CrossRef](#)]
20. Nguyen, K. D., Qiu, Y., Cui, X., Goh, Y. P., Mwangi, J., David, T., Mukundan, L., Brombacher, F., Locksley, R. M. and Chawla, A. 2011. Alternatively activated macrophages produce catecholamines to sustain adaptive thermogenesis. *Nature* **480**: 104–108. [[Medline](#)] [[CrossRef](#)]
21. Ohno, H., Shinoda, K., Spiegelman, B. M. and Kajimura, S. 2012. PPAR γ agonists induce a white-to-brown fat conversion through stabilization of PRDM16 protein. *Cell Metab.* **15**: 395–404. [[Medline](#)] [[CrossRef](#)]
22. Roskoski, R. Jr. 2018. The role of small molecule platelet-derived growth factor receptor (PDGFR) inhibitors in the treatment of neoplastic disorders. *Pharmacol. Res.* **129**: 65–83. [[Medline](#)] [[CrossRef](#)]
23. Saito, M., Okamatsu-Ogura, Y., Matsushita, M., Watanabe, K., Yoneshiro, T., Nio-Kobayashi, J., Iwanaga, T., Miyagawa, M., Kameya, T., Nakada, K., Kawai, Y. and Tsujisaki, M. 2009. High incidence of metabolically active brown adipose tissue in healthy adult humans: effects of cold exposure and adiposity. *Diabetes* **58**: 1526–1531. [[Medline](#)] [[CrossRef](#)]
24. Sakamoto, T., Takahashi, N., Sawaragi, Y., Naknukool, S., Yu, R., Goto, T. and Kawada, T. 2013. Inflammation induced by RAW macrophages suppresses UCP1 mRNA induction via ERK activation in 10T1/2 adipocytes. *Am. J. Physiol. Cell Physiol.* **304**: C729–C738. [[Medline](#)] [[CrossRef](#)]
25. Sakamoto, T., Nitta, T., Maruno, K., Yeh, Y. S., Kuwata, H., Tomita, K., Goto, T., Takahashi, N. and Kawada, T. 2016. Macrophage infiltration into obese adipose tissues suppresses the induction of UCP1 level in mice. *Am. J. Physiol. Endocrinol. Metab.* **310**: E676–E687. [[Medline](#)] [[CrossRef](#)]
26. Sam, S. and Mazzone, T. 2014. Adipose tissue changes in obesity and the impact on metabolic function. *Transl. Res.* **164**: 284–292. [[Medline](#)] [[CrossRef](#)]
27. Seki, T., Hosaka, K., Lim, S., Fischer, C., Honek, J., Yang, Y., Andersson, P., Nakamura, M., Näslund, E., Ylä-Herttua, S., Sun, M., Iwamoto, H., Li, X., Liu, Y., Samani, N. J. and Cao, Y. 2016. Endothelial PDGF-CC regulates angiogenesis-dependent thermogenesis in beige fat. *Nat. Commun.* **7**: 12152. [[Medline](#)] [[CrossRef](#)]
28. Sharp, L. Z., Shinoda, K., Ohno, H., Scheel, D. W., Tomoda, E., Ruiz, L., Hu, H., Wang, L., Pavlova, Z., Gilsanz, V. and Kajimura, S. 2012. Human BAT possesses molecular signatures that resemble beige/brite cells. *PLoS One* **7**: e49452. [[Medline](#)] [[CrossRef](#)]
29. Shin, W., Okamatsu-Ogura, Y., Machida, K., Tsubota, A., Nio-Kobayashi, J. and Kimura, K. 2017. Impaired adrenergic agonist-dependent beige adipocyte induction in aged mice. *Obesity (Silver Spring)* **25**: 417–423. [[Medline](#)] [[CrossRef](#)]
30. Sidossis, L. and Kajimura, S. 2015. Brown and beige fat in humans: thermogenic adipocytes that control energy and glucose homeostasis. *J. Clin. Invest.* **125**: 478–486. [[Medline](#)] [[CrossRef](#)]
31. Trayhurn, P. 2016. Recruiting Brown adipose tissue in human obesity. *Diabetes* **65**: 1158–1160. [[Medline](#)] [[CrossRef](#)]
32. Virakul, S., Dalm, V. A., Paridaens, D., van den Bosch, W. A., Mulder, M. T., Hirankarn, N., van Hagen, P. M. and Dik, W. A. 2015. Platelet-derived growth factor-BB enhances adipogenesis in orbital fibroblasts. *Invest. Ophthalmol. Vis. Sci.* **56**: 5457–5464. [[Medline](#)] [[CrossRef](#)]
33. Wang, Q. A., Tao, C., Gupta, R. K. and Scherer, P. E. 2013. Tracking adipogenesis during white adipose tissue development, expansion and regeneration. *Nat. Med.* **19**: 1338–1344. [[Medline](#)] [[CrossRef](#)]
34. Wu, J., Boström, P., Sparks, L. M., Ye, L., Choi, J. H., Giang, A. H., Khandekar, M., Virtanen, K. A., Nuutila, P., Schaart, G., Huang, K., Tu, H., van Marken Lichtenbelt, W. D., Hoeks, J., Enerbäck, S., Schrauwen, P. and Spiegelman, B. M. 2012. Beige adipocytes are a distinct type of thermogenic fat cell in mouse and human. *Cell* **150**: 366–376. [[Medline](#)] [[CrossRef](#)]
35. Yoneshiro, T., Aita, S., Matsushita, M., Okamatsu-Ogura, Y., Kameya, T., Kawai, Y., Miyagawa, M., Tsujisaki, M. and Saito, M. 2011. Age-related decrease in cold-activated brown adipose tissue and accumulation of body fat in healthy humans. *Obesity (Silver Spring)* **19**: 1755–1760. [[Medline](#)] [[CrossRef](#)]